IL NUOVO CIMENTO Vol. 31 C, N. 5-6 Settembre-Dicembre 2008
DOI 10.1393/ncc/i2009-10347-2

Numerical *vs.* turbulent diffusion in geophysical flow modelling

M. D'Isidoro(*), A. Maurizi and F. Tampieri
Istituto di Scienze dell'Atmosfera e del Clima (ISAC-CNR) - Bologna, Italy

(ricevuto il 20 Ottobre 2008; approvato il 30 Dicembre 2008; pubblicato online il 22 Giugno 2009)

Summary. — Numerical advection schemes induce the spreading of passive tracers from localized sources. The effects of changing resolution and Courant number are investigated using the WAF advection scheme, which leads to a sub-diffusive process. The spreading rate from an instantaneous source is compared with the physical diffusion necessary to simulate unresolved turbulent motions. The time at which the physical diffusion process overpowers the numerical spreading is estimated, and is shown to reduce as the resolution increases, and to increase as the wind velocity increases.

PACS 92.60.Sz – Air quality and air pollution.
PACS 92.60.hf – Tropospheric composition and chemistry, constituent transport and chemistry.
PACS 42.68.Bz – Atmospheric turbulence effects.
PACS 92.60.hk – Convection, turbulence, and diffusion.

1. – Introduction

Mixing is a property of turbulent geophysical flows that is represented in numerical simulations as a diffusion process. Diffusion is a symptom of the inability of models to simulate explicitly all the scales of motion. The importance of properly modelling the diffusion process for simulations of the Earth's system is beyond question.

Numerical simulations of geophysical flows are possible only after equations have been smoothed to remove the fine structure of the solutions, and smoothing implies the use of diffusion models.

The smoothing may be performed by averaging the Navier-Stokes equations over a grid box, which defines the space resolution of the simulation. Broadly speaking, the smoothing is the same as to applying a filter in the wave number space, retaining only small wave numbers. This procedure has recently been reviewed by Wingaard [1],

(*) E-mail: m.disidoro@isac.cnr.it

who introduces in the filtered equations a term, the deviatoric stress, that is due to the existence of non-zero velocity component correlations. Lilly [2] suggested that the simplest way to parameterise this term is by adapting an eddy viscosity model, based on the idea that the spatial scale of the grid lies in the inertial subrange of the spectrum of the velocity field solution. The earlier definition of a suitable diffusion coefficient was introduced by Smagorinsky [3], and was based on the Heisenberg assumption of the diffusive behaviour of the small scales, which are separated from the larger (resolved) ones.

As smoothing is done by ensemble averaging, the Reynolds equations are obtained and the velocity correlations must be parameterised. If a large enough separation in space and time exists between the explicitly resolved motions and the small-scale random-like velocities, the correlations between them become negligible, the common identification of "mean motion" and "turbulence" can be made, and the latter parameterised. In most geophysical problems, this separation, based on the existence of a spectral gap, is justified for the boundary layer dynamics (see [4], for instance) and, in particular, for the vertical component of velocity, whereas it is questionable in the troposphere, because the horizontal components of velocity do not show the gap (see [5]). Again, the simplest parameterisation is the assumption of flux-gradient relationships, with the definition of suitable diffusion coefficients.

From the numerical point of view, the need to inhibit the growth of instabilities in the solution for the dynamical fields may be satisfied in ways other than parameterising the physical diffusion due to unresolved scales. The numerical issue is tackled using hyperdiffusion terms and/or appropriate advection schemes. Note that passive tracers do not in principle need smoothing; numerical schemes that conserve the mass should be considered for a treatment consistent with an inviscid description. It is also known that different advection schemes induce numerical diffusion effects *per se*, even if no explicit smoothing is prescribed.

The present work is motivated by the necessity to assess the correct parameterisation of diffusion in air quality models. It concentrates on horizontal diffusion and addresses the issue of the competition between physical diffusion (due to the parameterisation of sub-grid motions) and numerical diffusion (intrinsic in the numerical scheme or induced by hyperdiffusion terms) for a given advection scheme. In particular, we consider the Weighted Average Flux (WAF) advection scheme [6] adopted in the BOLCHEM model [7] because of its mass conservation properties.

The paper is organized as follows. In sect. **2** a parameterisation of diffusion arising from unresolved turbulent motions is discussed, as a paradigm of physical dispersion. In sect. **3** the numerical aspects are dealt with. Subsequently, sect. **4** presents some numerical simulations for an idealized case, in order to establish a general frame for the evaluation of the numerical *vs.* physical effects of the diffusion. Finally, some conclusions are drawn.

2. – Sub-grid turbulent diffusion

In the present study the effect of unresolved (sub-grid) scales of turbulent motion on dispersion can be represented by a sub-grid turbulent diffusion coefficient D_H, where the subscript H emphasises the fact that only horizontal diffusion is considered. D_H can be estimated at a given resolution when the properties of turbulence at the scale of the resolution are known.

Assuming a Kolmogorov [8] spectrum, D_H as a function of the wave number is given by

$$D_H(k) = \frac{9}{2}\frac{C_1^2}{C_0}\varepsilon^{1/3}k^{-4/3}\,, \tag{1}$$

where $C_1 = 0.25C_K$ ($C_K = 2$), $C_0 = 6.2$ is the Lagrangian structure function constant, and ε can be determined from velocity spectra measured in a variety of flow conditions and experimental arrangements. Following [9], in the boundary layer ($z < h$) we have

– unstable conditions [10]:

$$\varepsilon = \frac{u_*^3}{\kappa\tilde{z}}\left(0.61 - 1.75\frac{\tilde{z}}{L_{MO}}\right), \quad L_{MO} < 0; \tag{2}$$

– stable conditions [11]:

$$\varepsilon = \frac{u_*^3}{\kappa\tilde{z}}\left(0.61 - 5\frac{\tilde{z}}{L_{MO}}\right), \quad L_{MO} > 0 \tag{3}$$

where $\tilde{z}^{-1} = \ell_0^{-1} + z^{-1}$ in which $\ell_0 = 500\,\mathrm{m}$ is assumed; and L_{MO} is the Monin-Obukhov length.

Above the boundary layer ($z > h$) $\varepsilon = 5. \times 10^{-5}\,\mathrm{m^2\,s^{-3}}$ is assumed as being representative of tropospheric data. For model applications, the height h can be determined case by case, using model profiles along with the actual stability.

As an example, in free-troposphere for a grid mesh size $\Delta x = 10\,\mathrm{km}$, the Tampieri and Maurizi [9] model gives $D_H = 310\,\mathrm{m^2\,s^{-1}}$.

3. – Remarks on numerics

Let us consider the advection equation for the concentration $C(\mathbf{x}, t)$ of a passive tracer:

$$\left(\frac{\partial}{\partial t} + \mathbf{U}\cdot\nabla\right)C = 0, \tag{4}$$

where $\mathbf{U}$ is the prescribed velocity field.

The discretisation of eq. (4) produces, in general, the spread of a cloud of tracer advected by the velocity field (see, *e.g.*, [12]). The nature and magnitude of this spread is not only a function of the resolution, but also of the numerical scheme. For simplicity, the spread is referred to as numerical diffusion, regardless of the fact that the process may display or not diffusive behaviour, *i.e.* a growth of the cloud size σ proportional to the square root of time.

3˙1. *Non-dimensional form of advection equation.* – In order to identify the parameters relevant to the study of numerical diffusion, the source dimension R and the characteristic wind speed U are selected as scales for length and velocity, respectively, to give eq. (4) the non-dimensional form

$$\left(\frac{\partial}{\partial t'} + \frac{UT}{R}\mathbf{U}'\cdot\nabla'\right)C' = 0, \tag{5}$$

where the prime indicates non-dimensional quantities and operators. The time scale must be defined as $T = RU^{-1}$ to make eq. (5) scale invariant.

In order to solve eq. (5) numerically, space and time are discretised by Δx and Δt, respectively. Combining the non-dimensional grid mesh size $\Delta x' = R^{-1}\Delta x$ and time step $\Delta t' = UR^{-1}\Delta t$, we define the following set of non-dimensional parameters: the resolution

$$\rho = \frac{R}{\Delta x} \equiv (\Delta x')^{-1} \tag{6}$$

and the Courant number

$$\nu = \frac{\Delta t U}{\Delta x} \equiv (\Delta t')(\Delta x')^{-1}\,. \tag{7}$$

Using these parameters, the non-dimensional time is expressed by

$$t' = N\nu\rho^{-1}, \tag{8}$$

where $N = t\Delta t^{-1}$ represents the number of integration steps.

Any solution of eq. (5) depends on two parameters only, as does the increase in variance σ^2 of the tracer distribution $C(\mathbf{x}, t)$ with respect to its initial value, which in non-dimensional terms, reads

$$\Delta\sigma'^2(t'; \rho, \nu) = \frac{\sigma^2(t') - \sigma^2(t_0)}{R^2}\,. \tag{9}$$

3˙2. *Weighted-average flux advection scheme.* – In the present study use is made of a mass conservative advection algorithm based on the WAF numerical scheme [6], which is briefly described below.

The advection equation (4) is solved numerically using an operator splitting approach, namely, by carrying out the computations for each of the space dimensions sequentially. Discretising in i-th direction in space one obtains

$$C_i^{n+1} = C_i^n - \frac{\Delta t}{\Delta x_i}(f^*_{i+1/2} - f^*_{i-1/2}), \tag{10}$$

where f^* is the numerical WAF flux [13] defined as

$$f^*_{i+1/2} = \frac{1}{2}(1 + \phi_{i+1/2})f_i + \frac{1}{2}(1 + \phi_{i-1/2})f_{i+1} \tag{11}$$

and ϕ_i are "limiter functions", which have in general the form of an amplification factor applied to the Courant number ν.

In order to eliminate undesired oscillations from the solution, the limiter functions are defined to be function also of the local flow parameter $r = \Delta C_{\text{upwind}}/\Delta C_{\text{local}}$, which avoids spurious oscillations by adding a numerical dissipation. The limiter functions are defined as

$$\phi(r, \nu) = \text{sgn}(\nu)[1 + (|\nu| - 1)b], \tag{12}$$

TABLE I. – *Summary of the numerical experiments performed, showing parameters ρ and ν, time step length Δt and horizontal velocity component U. Experiments are organised in groups (A to F), each characterised by a given ρ. The suffix numbers indicate the values of ρ and ν, respectively, used for each experiment.*

Experiment	ρ	ν	U(m/s)	Δt(s)
$A_{\rho 5,\nu 0.04}$	5	0.04	1	100
$A_{\rho 5,\nu 0.8}$	5	0.8	20	100
$B_{\rho 3.33,\nu 0.026}$	3.33	0.026	1	100
$C_{\rho 2.5,\nu 0.04}$	2.5	0.04	1	100
$D_{\rho 1.65,\nu 0.013}$	1.65	0.013	1	100
$E_{\rho 1.25,\nu 0.01}$	1.25	0.01	1	100
$F_{\rho 0.5,\nu 0.004}$	0.5	0.004	1	100
$F_{\rho 0.5,\nu 0.08}$	0.5	0.08	20	100

where

$$b = \max[0, \min(2r, 1), \min(r, 2)]. \tag{13}$$

Given the above hypotheses, the resulting WAF advection scheme is second-order accurate in space (first in time), and is conservative for divergence-free wind fields.

4. – Results and discussion

In order to evaluate the effect of numerical diffusion, several numerical tests were performed for different grid resolutions and Courant numbers. A simplified framework was chosen, with wind field $(u, v) = (U, 0)$, in order to single out the effects of sub-grid processes. The initial tracer distribution was chosen with Gaussian-shape and standard deviation $\sigma_0 = R$. Aiming to measure the effect of numerical diffusion as a function of the mass distribution resolution, the numerical tests were set up varying the two parameters ρ and ν. Experiments are summarised in table I.

Figure 1 shows the increase of normalised puff variance with non-dimensional time for different values of ρ (a) and ν (b). Variations of ρ induce large variations of $\Delta\sigma'^2$, while varying ν does not have a strong impact, being practically negligible for low resolutions. Although for the largest resolution the differences induced by variations of ν are not so small (see the two lowest curves in fig. 1b), this parameter is neglected hereinafter.

For large nondimensional time, say $\mathcal{O}(100)$, it can be assumed that the increase of variance with time can be well approximated by a power law:

$$\Delta\sigma'^2 = \alpha t'^{\beta}. \tag{14}$$

Fitting eq. (14) on data allows the determination of both slope β and "diffusion coefficient" α. The results are reported in figs. 2a and 2b for different ρ.

Although β varies between 0.3 and 0.4 in the range of ρ considered, its variation is small, and this justifies the direct comparison of α in fig. 2a.

In all cases the representative value of β corresponds to a sub-diffusive process. The magnitude of this process is largely driven by resolution, as shown in fig. 2a, where the sub-diffusion coefficient α varies by orders of magnitude with ρ. This suggests that

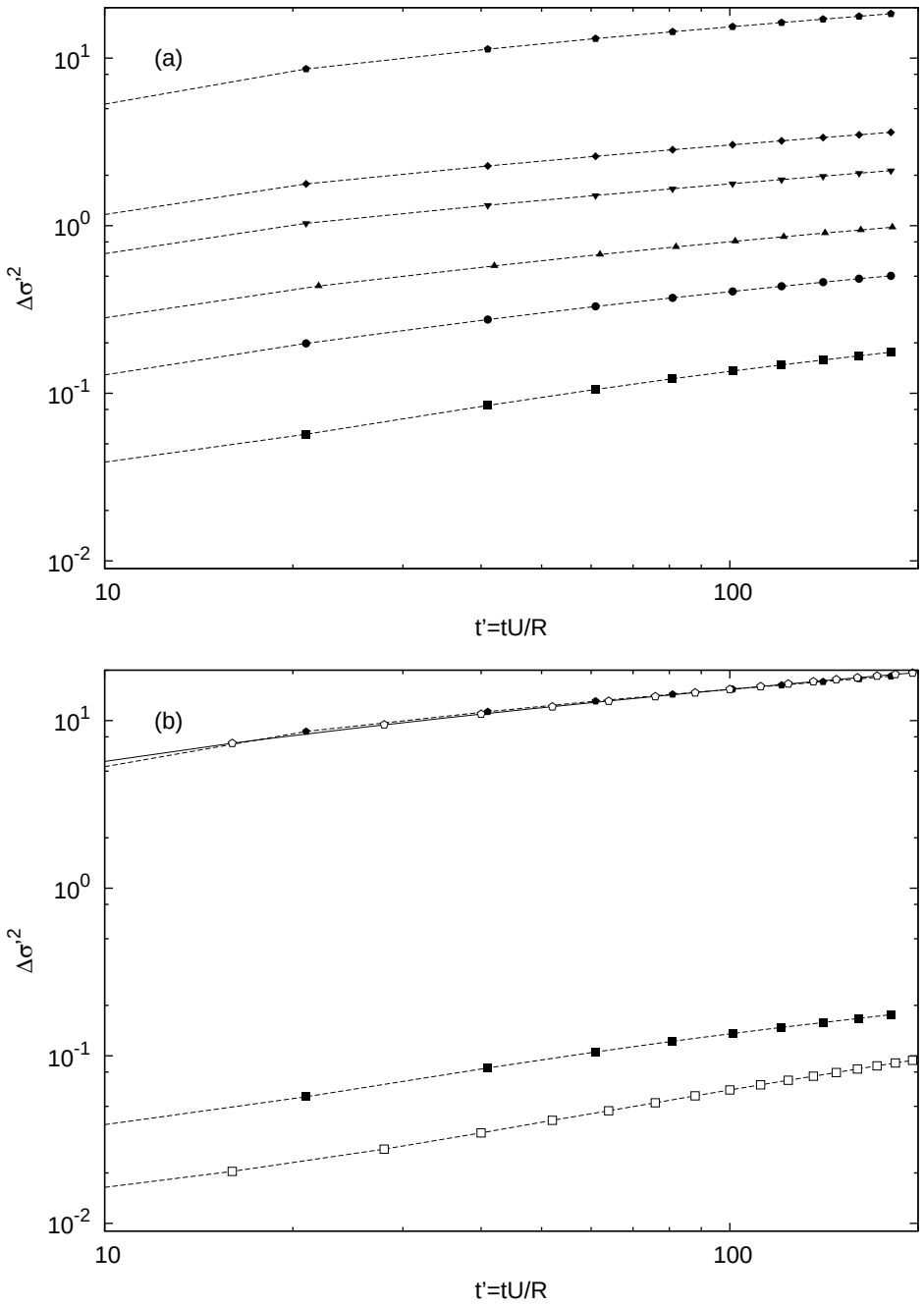

Fig. 1. – (a) Normalised variance as a function of non-dimensional time t' for different values of ρ: starting from top to bottom the curves refer to experiments $A_{\rho 5,\nu 0.04}$, $B_{\rho 3.33,\nu 0.026}$, $C_{\rho 2.5,\nu 0.04}$, $D_{\rho 1.65,\nu 0.013}$, $E_{\rho 1.25,\nu 0.01}$ and $F_{\rho 0.5,\nu 0.004}$, respectively. (b) The same as (a) but for experiments with the same ρ and different values of ν: $F_{\rho 0.5,\nu 0.004}$ and $F_{\rho 0.5,\nu 0.08}$, black and white circles, respectively; $A_{\rho 5,\nu 0.04}$ and $A_{\rho 5,\nu 0.8}$, black and white squares, respectively.

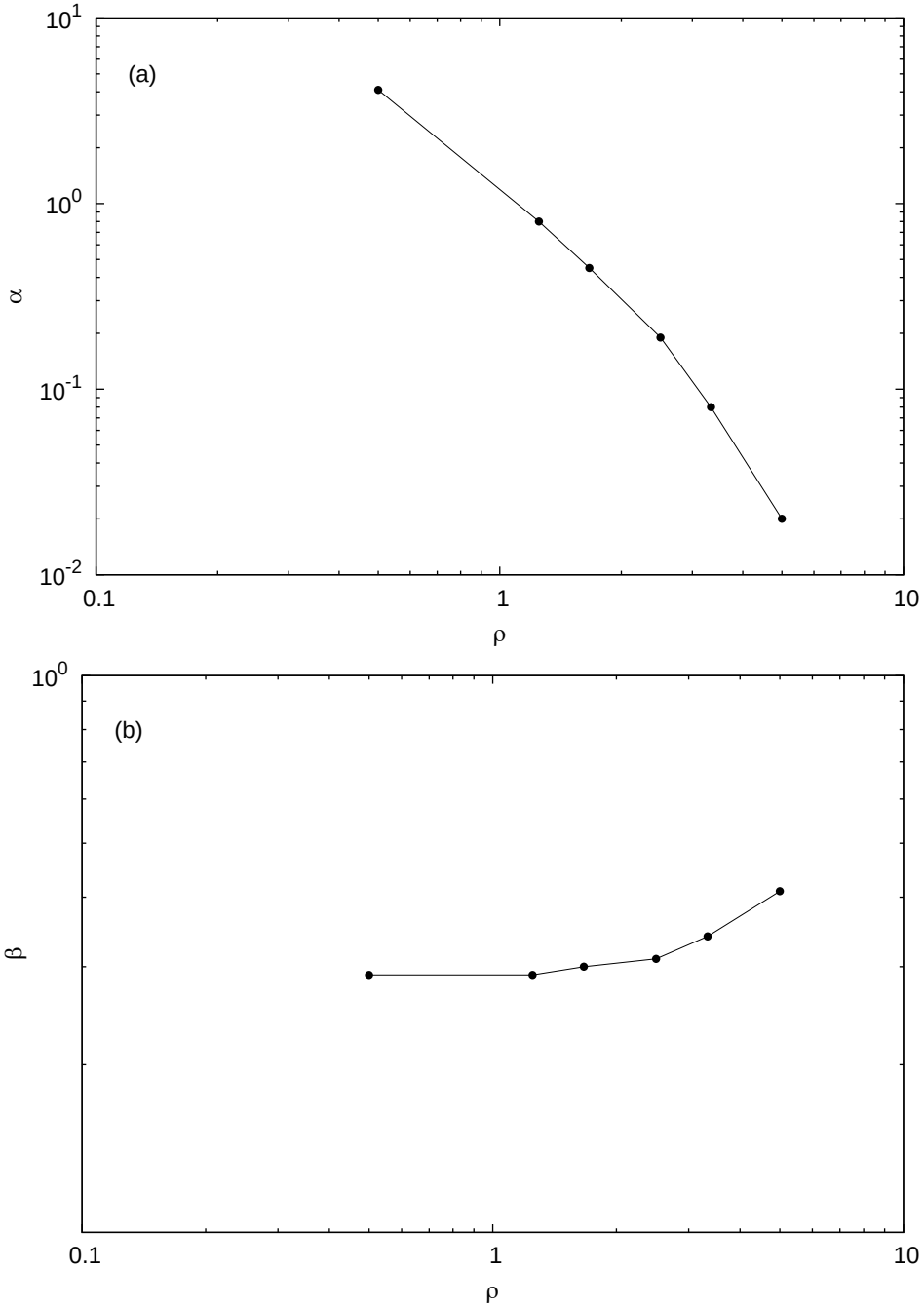

Fig. 2. – Coefficients α (a) and exponent β (b) of eq. (14), as a function of ρ.

conditions can be met for physical diffusion ($\propto t'$) to become dominant, depending on the numerical resolution.

In order to give an idea of what those conditions are, a direct comparison with the sub-grid turbulent diffusion described in sect. **2** was performed.

The turbulent diffusion was modelled assuming an Ornstein-Uhlenbeck process [14], which is equivalent to a diffusion process in Gaussian, steady, homogeneous turbulent conditions. Use was made of the values for the variance and the dissipation rate of turbulent flow according to sect. **2**, based on the resolution adopted for the numerical solution of eq. (4).

The increase of non-dimensional variance for the turbulent (Lagrangian) diffusion process is expressed by

$$\Delta\sigma_L'^2 = \frac{2Dt}{R^2} = 2D't', \tag{15}$$

where $D' = D(RU)^{-1}$ is the non-dimensional sub-grid diffusion coefficient, which is a function of Δx. Assuming that the wave number is $k = \pi(\Delta x)^{-1}$, from eq. (1) it can be expressed by

$$D'_H = \gamma \frac{(\varepsilon R)^{1/3}}{U} \rho^{-4/3}, \tag{16}$$

where $\gamma = (9/2)\pi^{-4/3}(0.25C_K)^2 C_0^{-1}$. Note that since the turbulent dispersion process does not depend on U and R, the non-dimensionalisation makes D'_H explicitly dependent on them. Therefore, in order to compare the results of the numerical and turbulent processes, R and U must be selected. Here R, representing the source scale, is given a fixed value, $\tilde{R} = 12500\,\mathrm{m}$, while U is left to vary. It can be observed that this makes ν vary from case to case, although due to its limited impact on numerical diffusion, the results are compared considering ρ only.

Figures 3a, b, c and d show $\Delta\sigma_L'^2(\tilde{R}, U)$ for different resolutions ($\rho = 0.5$, 1.25, 3.33, 5, respectively), each for different values of U, along with $\Delta\sigma'^2$ for comparison.

The intersection between $\Delta\sigma'^2$ and $\Delta\sigma_L'^2(\tilde{R}, U)$ defines the time at which turbulent diffusion starts to dominate over numerical sub-diffusion. Increasing resolution reduces both variances but, due to the different dependence on ρ, the numerical sub-diffusion coefficient declines more rapidly than the turbulent diffusion coefficient. This makes high-resolution simulations more sensitive to turbulence parameterisation. Furthermore, for low wind velocity it occurs in a shorter time. In fact, in the limit $U \to 0$, the numerical effects on diffusion vanish.

The time τ at which the dimension of the puff is equal for the numerical and turbulent diffusion processes can be computed using eq. (14) and eq. (15) by

$$\tau = \left(\frac{2D'(\rho, \tilde{R}, U)}{\alpha(\rho)} \right)^{(\beta-1)^{-1}}. \tag{17}$$

Figure 4 reports τ, as a function of ρ for different U (for given $\tilde{R}$). Wind velocity has a major role in determining τ, especially for resolutions below 2.5. For higher resolutions however, τ decreases rapidly.

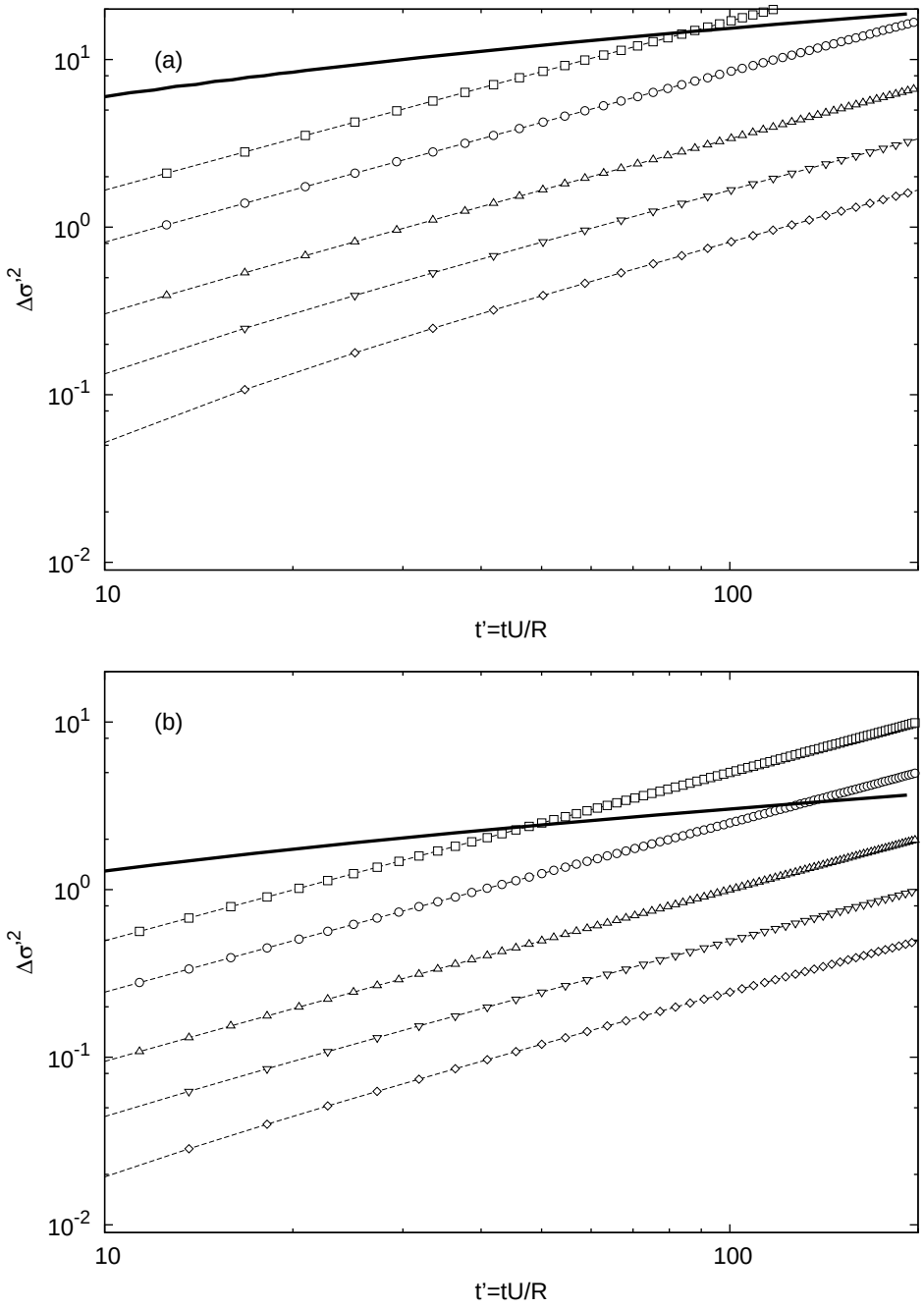

Fig. 3. – Comparison of numerical (continuous line) and physical diffusion for different wind velocities, for four resolutions: (a) $F_{\rho 0.5,\nu 0.004}$; (b) $E_{\rho 1.25,\nu 0.01}$; (c) $B_{\rho 3.33,\nu 0.026}$ and (d) $A_{\rho 5,\nu 0.04}$. Lines with symbols are, from top to bottom, for $U = 1, 2, 5, 10, 20\,\mathrm{ms}^{-1}$.

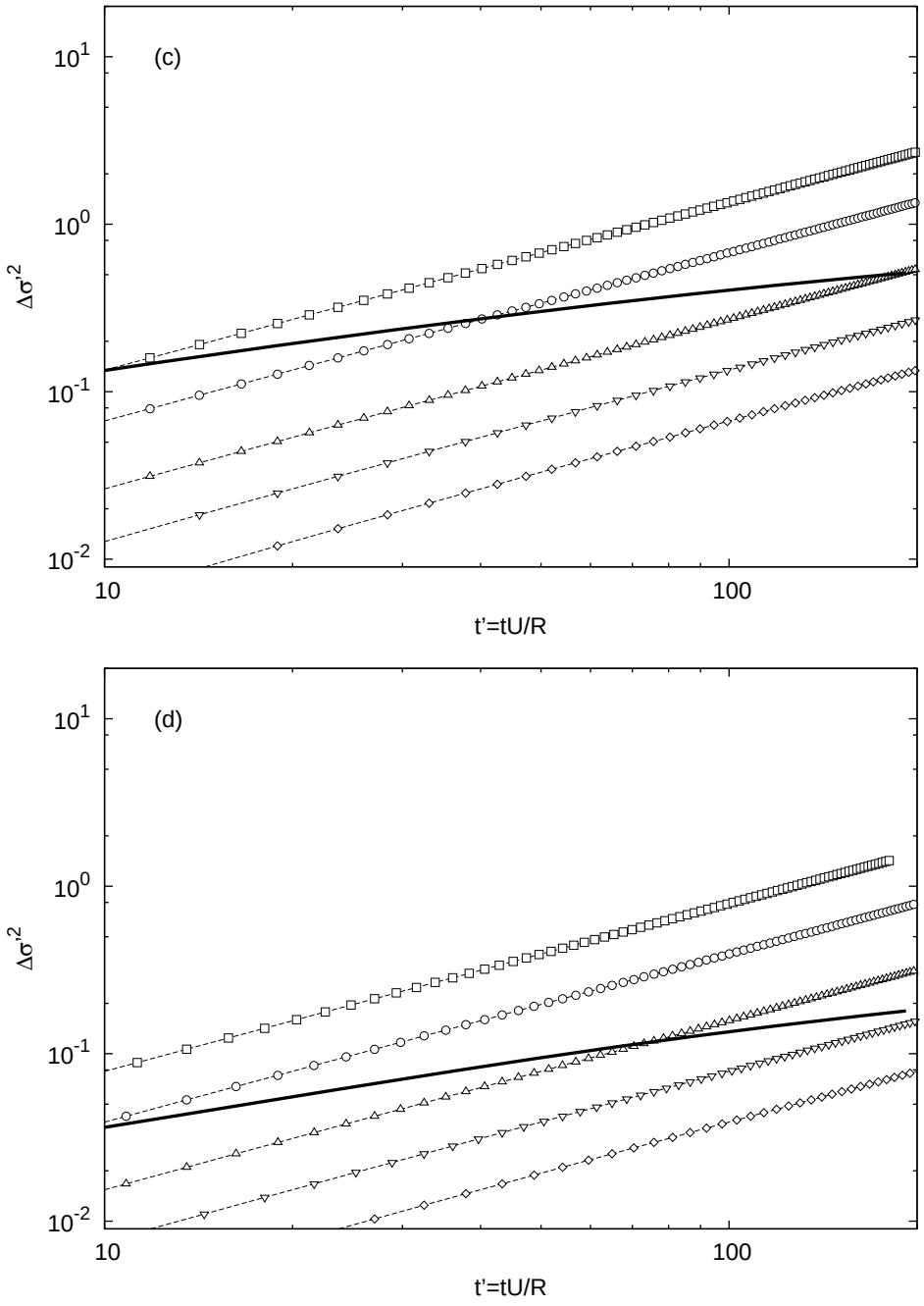

Fig. 3. – (*Continued*).

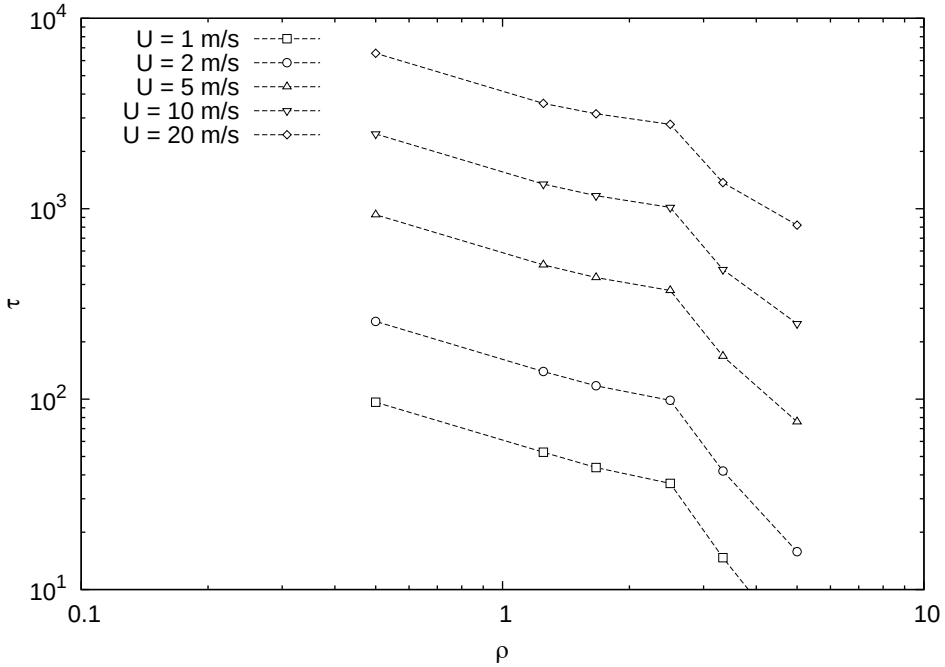

Fig. 4. – Time τ as a function of ρ, computed for different velocities U.

5. – Conclusions

The present paper has considered the horizontal spread of a tracer released istantaneously in a uniform wind field, to study the diffusion induced by the numerical advection scheme WAF in comparison with the sub-grid physical diffusion. It has been found that

- numerical diffusion depends on only two parameters: resolution and Courant number;
- while resolution plays a major role, variations due to the Courant number are negligible;
- numerical spread induced by WAF is subdiffusive;
- the time at which physical diffusion starts to be larger than numerical diffusion decreases as the resolution increases;
- the said time is further reduced in low wind conditions.

With the present value of the source size R and for grid mesh size between 5 and 20 km the numerical diffusion overpowers the physical one for few hours to days. Thus the gradients are excessively smoothed and there is no room for a more physical description of the dispersion process.

However, extrapolating the results for τ to finer grid mesh sizes ($\sim$ 1 km) the role of physical diffusion is likely to become more and more important. This requires the

extension of the present study to the range of resolution ρ between 5 and 20, going in the range attainable by non-hydrostatic models.

Another remark is in order regarding air quality simultations: the resolution ρ is always about 1 because scales of sources are much smaller than the grid mesh size. This means that in this kind of simulations, numerical diffusion is always dominating over the physical one. Further investigations on less diffusive advection schemes is therefore mandatory.

* * *

The authors would like to thank P. MALGUZZI for his valuable support. M. D'ISIDORO was supported by the FP6 IP GEMS. Partial support from the Italia-USA Cooperation Agreement on Science and Technology of Climate Change is also acknowledged.

REFERENCES

[1] WYNGAARD J. C., *J. Atmos. Sci.*, **61** (2004) 1816.
[2] LILLY D. K., *On the application of the eddy viscosity concept in the inertial subrange of turbulence*, NCAR Tech. Rep. 123, National Center for Atmspheric Research (1966).
[3] SMAGORINSKY J., *Mon. Weather Rev.*, **91** (1963) 99.
[4] COURTNEY M. and TROEN I., *Wind speed spectrum from one year of continuous 8 hz measurements*, in *Proceedings of the 9th Symposium on Turbulence and Diffusion*, (American Meteorological Society, Boston, Mass.) 1990, pp. 301–304.
[5] GAGE K. S., *Dynamic processes contributing to the mesoscale spectrum of atmospheric motions*, in *Atmospheric Turbulence and Mesoscale Meteorology*, edited by FEDOROVICH E., ROTUNNO R. and STEVENS B. (Cambridge University Press) 2004, pp. 223–263.
[6] BILLET S. J. and TORO E. F., *J. Comput. Phys.*, **130** (1997) 1.
[7] MIRCEA M., D'ISIDORO M., MAURIZI A., VITALI L., MONFORTI F., ZANINI G. and TAMPIERI F., *Atmos. Environ.*, **42** (2008) 1169.
[8] KOLMOGOROV A. N., *Dokl. Akad. Nauk SSSR*, **30** (1941) 301.
[9] TAMPIERI F. and MAURIZI A., *Nuovo Cimento C*, **30** (2007) 395.
[10] ALBERTSON J. D., PARLANGE M. B., KIELY G. and EICHINGER W. E., *J. Geophys. Res. D*, **102** (1997) 13423.
[11] PAHLOW M., PARLANGE M. B. and PORTE-AGEL F., *Boundary-Layer Meteorol.*, **99** (2001) 225.
[12] SMOLARKIEWICZ P. K., *J. Comput. Phys.*, **54** (1984) 325.
[13] HUBBARD M. E. and NIKIFORAKIS N., *Mon. Weather Rev.*, **131** (2003) 1848.
[14] GARDINER C. W., *Handbook of Stochastic Methods for Physics, Chemistry and the Natural Sciences* (Springer-Verlag) 1990, second edition.